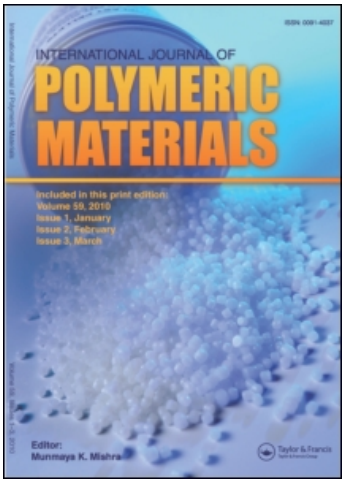

International Journal of Polymeric Materials
Publication details, including instructions for authors and subscription information:
http://www.informaworld.com/smpp/title~content=t713647664

Some Methods of Experimental Studies into the Extension of Polymeric Liquids

A. N. Prokunin[a]
[a] Institute for Problems in Mechanics, USSR Academy of Sciences, Moscow, USSR

To cite this Article Prokunin, A. N.(1980) 'Some Methods of Experimental Studies into the Extension of Polymeric Liquids', International Journal of Polymeric Materials, 8: 4, 303 — 321
To link to this Article: DOI: 10.1080/00914038008077957
URL: http://dx.doi.org/10.1080/00914038008077957

Intern. J. Polymeric Mater., 1980, Vol. 8, pp. 303–321
0091–4037/80/0804–0303 $06.50/0

Printed in Great Britain

Some Methods of Experimental Studies into the Extension of Polymeric Liquids†

A. N. PROKUNIN
Institute for Problems in Mechanics, USSR Academy of Sciences, Moscow, USSR

(*Received in final form February 25, 1980*)

Experimental studies into the extension of polymeric liquids have revealed an envelope in the stress versus recoverable strain relationships, flow retardation under considerable elastic strains, and a correlation between uniform and non-uniform extensions.

1. INTRODUCTION

This three-part work is concerned with some methods of experimental studies into the extension of polymer melts.

The first part deals primarily with the properties of the stress-recoverable strain relationships derived at uniform extension and the envelope featured by these relationships.

The second part concerns the correlation between uniform and non-uniform extensions, frequently occurring in polymer processing.

The third part covers the retardation of polymeric liquid flows, which is established by direct measurements of the nonrecoverable strain rate at uniform extension. This experiment has been carried out in collaboration with N. N. Filippova.

The first two parts of this work have involved experiments with polyisobutylene P-20, while the third, mainly low-density polyethylene (some qualitative experiments have been conducted using high-density polyethylene and polystyrene).

† Presented at the 10th All-Union Symposium on Polymer Rheology, June 20–24, 1978, Perm, USSR.

2. UNIFORM EXTENSION

2.1 Some definitions

The uniform inertialess extension of a cylindrical specimen is characterized by the following rate components:

$$V_x = \kappa(t)x; \qquad V_r = -\frac{\kappa(t)}{2}r; \qquad V_\phi \equiv 0. \tag{1}$$

Here, x, r and ϕ are cylindrical coordinates (the x axis runs along the specimen), and $\kappa(t)$ is the strain rate dependent, in the general case, on time t ($\kappa \geqslant 0$).

In the experiments, force F is either measured or predetermined, while the stress which is constant throughout across the specimen is determined as follows:

$$\sigma = F/P, \tag{2}$$

where P is the cross-sectional area of the specimen.

The unit elongation of an incompressible specimen is

$$\varepsilon = l/l_0 = r_0^2/r^2. \tag{3}$$

In Exp. (3), l_0 and r_0 are the specimen length and radius, respectively, at the onset of straining, while l and r are the same parameters at any other instant of extension. The second equality in Exp. (3) stems from the incompressibility of the medium.

In accordance with the known relationship between total strain ε and time t, strain rate κ is determined from the formula

$$\kappa = \frac{\mathrm{d}}{\mathrm{d}t}(\ln \varepsilon). \tag{4}$$

Taken as a measure of elastic (recoverable) strain is

$$\alpha = l/l_r. \tag{5}$$

Here, l_r is the length which a piece of the extended specimen having length l tends to assume after the tensile stress is instantaneously removed at $t \to \infty$. The contraction is caused by the elastic energy accumulated when the polymeric liquid is extended.

As the amount of nonrecoverable strain (β)

$$\beta = l_r/l_0 = \varepsilon\alpha; \qquad \ln \beta = \ln \varepsilon - \ln \alpha \tag{6}$$

is usually taken.[1] Then, the nonrecoverable strain rate is determined as:

$$e_p = \frac{\mathrm{d}}{\mathrm{d}t}(\ln \beta). \tag{7}$$

Along with the extension processes this work is also concerned with stress relaxation. To provide for stress relaxation, the extension of the specimen is

discontinued instantaneously, and stress σ starts decreasing with time t. In this case, the length and diameter of the specimen remain invariable in time.

Experimentally examined in this work is uniform extension at constant strain rate κ and constant force F.

In the case where $\kappa = \text{const}$, Exps. (1) and (2) suggest that

$$r = r_0 \exp(-\kappa t/2); \qquad \sigma = \frac{F}{P_0} \exp(-\kappa t), \tag{8}$$

where P_0 is the cross-sectional area of the specimen at $t = 0$.

In the case of extension with $F = \text{const}$, the relation between σ and ε is as follows:

$$\sigma = \sigma_0 \varepsilon; \qquad \sigma_0 = F/P_0. \tag{9}$$

2.2 Experimental

A melt of polyisobutylene P-20 (molecular weight, ca 10^5; specific density, $9.2 \cdot 10^2$ kg/m^3) was investigated at 22°C. The maximum (Newtonian) viscosity of the polymer is $\eta \approx 1.1 \cdot 10^6$ Pa.s. The equilibrium high-elastic modulus[1] is $G_e \approx 1.5 \cdot 10^3$ Pa. Viscosity η and modulus G_e were determined in the region of linear behavior of the liquid at shear and tension.[1]

Experiments with $\kappa = \text{const}$ were conducted using a setup with both variable[2] and invariable length of the specimen. In the latter case, one end of the specimen was stationary, while the other was wound on a pulley.[3] The setup using an invariable-length specimen was used to attain high values of ε.

Cylindrical polyisobutylene specimens were prepared by rolling the polymer out between two glass plates to the required diameter. The latter was preset by means of two balls of a given size. The tension specimens were usually made with radius $r_0 \approx 0.3$ cm. Such a technique has made it possible to prepare specimens of a shape differing from the cylindrical one by less than 3% as measured along the radius.

Both the pulley[3] and the movable clamp[2] of the setup could be instantaneously immobilized, after which the decrease in stress with time (stress relaxation) was measured.

On setups with constant and variable specimen length, the following strain rates were achieved: $2.84 \cdot 10^{-4}$, $1.2 \cdot 10^{-3}$, $3.84 \cdot 10^{-2}$, $1.2 \cdot 10^{-3}$, $3.84 \cdot 10^{-2}$, 10 s^{-1}, as well as strains ε of up to 40. The limitations on ε were imposed by the specimen inhomogeneity resulting from significant strains.

In tensile tests with $\kappa = \text{const}$, the following parameters were measured as a function of time t: tensile force F, total strain ε (hence, specimen radius r and stress σ), and recoverable strain α.

The scatter in experimental data was substantial, as great as $\pm 15\%$ at high strains.

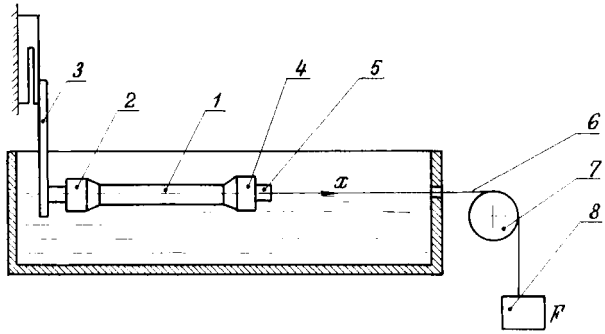

FIGURE 1 Setup for uniform extension with a constant force.

The extension with constant force F and stress relaxation (after extension with F = const) in cylindrical specimens with initial radius r_0 were carried out using a setup shown schematically in Figure 1. The left end of specimen 1 was attached via bushing 2 to the outer plate of capacitive transducer 3. The right end was secured, by means of a similar bushing 4, to float 5 on the surface of water. The water bath was intended to compensate for the specimen's weight and to provide for temperature control. Attached to the float was thread 6 passing through pulley 7 and suspending weight 8. Normally, such an arrangement (particularly when the pulley is replaced by a cylinder over which the thread slides) may cause spontaneous vibration of the specimen at great elongations. Therefore, the experiments were repeated, whenever possible (when the specimen was much lighter than the weight), with the specimen being extended vertically without any pulley.

In stress relaxation measurements, a fork was installed at an appropriate distance, checking the movement of the float, after which the relaxation process began.

Measured during the experiment were tensile force F, total strain $\varepsilon = l/l_0$ (length l was preset visually by moving the float along a ruler), and recoverable strain α.

The experiments were conducted at $\sigma_0 = (1, 3.3, 6.3, 11.7)\cdot 10^3$ N/m^2. The scatter in experimental data at $\varepsilon < 10$ did not exceed $\pm 10\%$ but became more pronounced when ε was measured in the region of its sharp increase (see Figure 3).

The homogeneity of the specimens was checked in all experiments by local photography. The experiments which were considered to be satisfactory were those in which the deviation of the calculated radiuses (see Exps. (3) and (8)) from the photographed ones did not exceed 5%.

Also measured was recoverable strain $\alpha = l/l_r$ under all straining conditions. To this end, a piece having length l was cut off from the specimen with

scissors, then the cut-off piece contracted afloat for about an hour[1] with subsequent measurement of length l_r.

More details regarding the measurement procedure will be given below in the discussion of the experimental results.

2.3 Experimental results and their discussion

The curves representing relation $\sigma/\kappa\eta$ and recoverable strain α versus time t in the case of extension at a constant strain rate for different values of κ are shown in Figure 2a, b.

At $\kappa \leqslant 3.84 \cdot 10^{-3}\ s^{-1}$, steady flow was experimentally attained. Extension with $\kappa = 3.84 \cdot 10^{-4}\ s^{-1}$ corresponds to linear behavior of the fluid. Effective viscosity σ/κ and recoverable strain α at steady flow increase with κ, which has been reported earlier in Refs. 2 and 4. It should also be noted that the greater the value of κ, the sooner (with respect to τ) the steady flow is attained.

In the case of $\kappa > 3.84 \cdot 10^{-3}\ s^{-1}$, the steady flow was not achieved, but whether this is a rheological property of the examined polyisobutylene or a result of the above-mentioned limitations imposed on ε by the setup is difficult to tell.

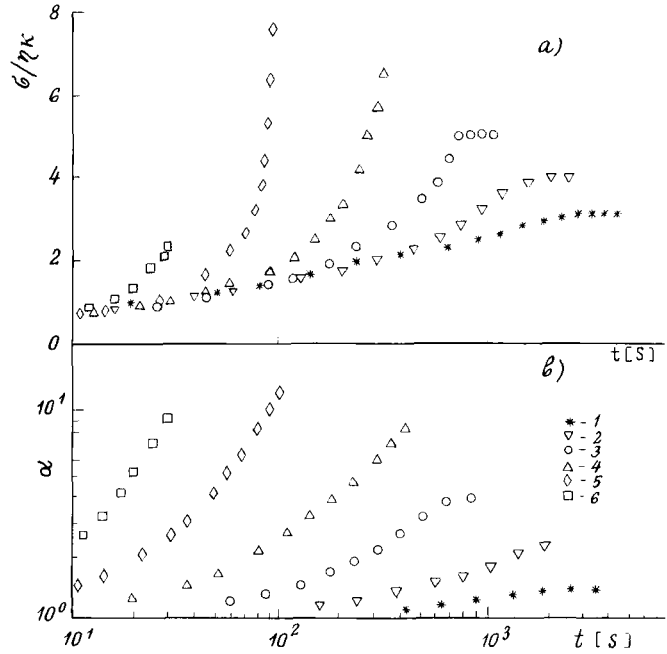

FIGURE 2 Uniform extension at constant strain rate κ. $\sigma/\kappa\eta$ (a) and recoverable strain α (b) versus time t. Corresponding to points 1 through 6 are $\kappa = 3.84 \cdot 10^{-4}$, $1.2 \cdot 10^{-3}$, $3.84 \cdot 10^{-3}$, $1.2 \cdot 10^{-2}$, $3.84 \cdot 10^{-2}$, and $10^{-1}\ s^{-1}$.

The curves representing total strain $\varepsilon = l/l_0$ and recoverable strain α versus time t in the case of extension with constant force F for different initial stresses $\sigma_0 = F/P_0$ (P_0 is the cross-sectional area of the specimen prior to straining) are given in Figure 3a, b. In the region of t under consideration, the experimental curves are monotonically increasing relations, the increase being proportional to that in σ_0. Note that the $\varepsilon(t)$ curve for an elastic liquid is higher than that for a Newtonian liquid of the same viscosity.

The stress σ versus recoverable strain α curves are presented in Figures 4 and 5.

The white symbols in Figure 4a correspond to the $\sigma(\alpha)$ curve at extension with different constant strain rates. These curves have been derived from the experimental data of Figure 2a, b. For $\kappa \lesssim 3.84 \cdot 10^{-3}$ s^{-1}, the last white symbol (the circle corresponding to maximum α) corresponds to steady

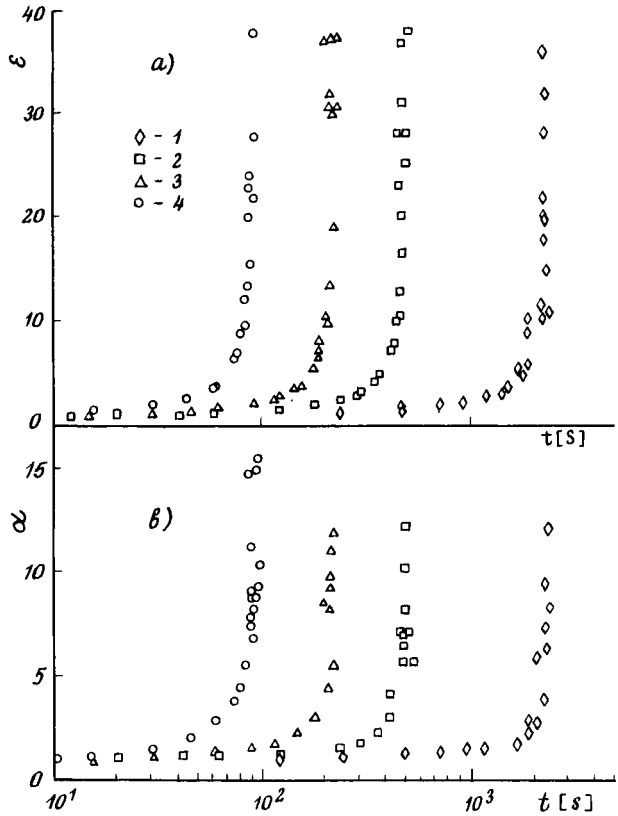

FIGURE 3 Uniform extension with a constant force. Strain ε (a) and recoverable strain α (b) versus time t. Corresponding to points 1 through 4 are $\sigma_0 = (1, 3.3, 6.3, 11.7) \cdot 10^3$ N/m^2.

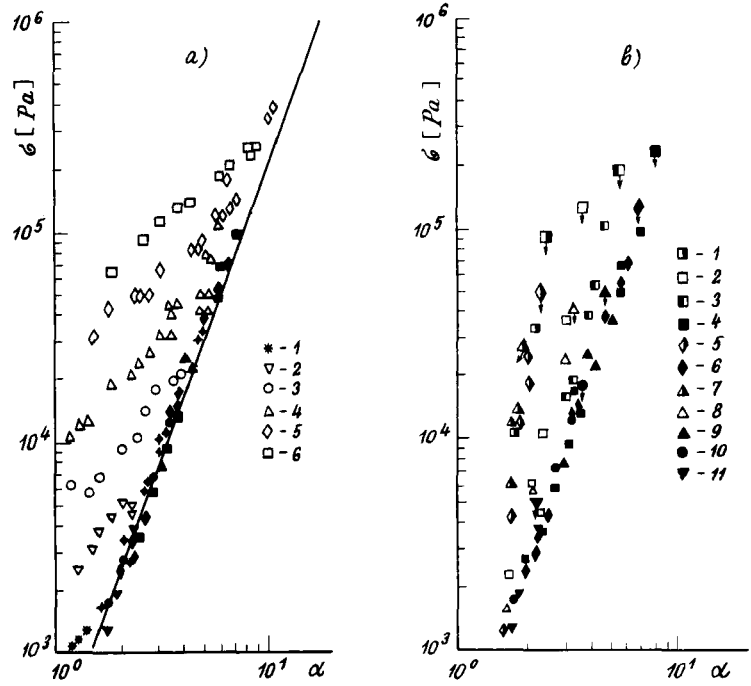

FIGURE 4 (a) Tensile stress σ versus recoverable strain α at extension with κ = const. Corresponding to points 1 through 6 are $\kappa = 3.84 \cdot 10^{-4}$, $(1.2, 3.84) \cdot 10^{-3}$, $(1.2, 3.84) \cdot 10^{-2}$, and $10^{-1}\ s^{-1}$. Black symbols represent the envelope for these relationships. (b) Stress σ versus α in the case of stress relaxation after extension. Corresponding to points 1 through 4 are $\kappa = 10^{-1}\ s^{-1}$ and $\ln \varepsilon = 1.3$, 1.8, 2.35 and 2.9; corresponding to points 5 and 6 are $\kappa = 3.84 \cdot 10^{-2}\ s^{-1}$ and $\ln \varepsilon = 1.15$ and 2.9; corresponding to points 7 through 9 are $\kappa = 1.2 \cdot 10^{-2}\ 2^{-1}$ and $\ln \varepsilon = 1.3$, 2.16 and 2.9; and corresponding to point 11 are $\kappa = 1.2 \cdot 10^{-3}$ and $\ln \varepsilon = 2.6$.

flow. As can be seen from Figure 4a, stress σ depends not only on α but also on strain rate κ. Both relations are nonlinear with respect to α and κ, since

$$\frac{\partial^2 \sigma}{\partial \kappa^2} < 0; \qquad \frac{\partial^2 \sigma}{\partial \alpha\, \partial \kappa} > 0.$$

The white symbols in Figure 5a correspond to the $\sigma(\alpha)$ curve at extension with different forces (initial stresses σ_0). These curves have been constructed from the experimental values presented in Figure 3a, b. Figure 5a shows that the experimentally obtained $\sigma(\alpha)$ curves converge as α increases. Comparison of the $\sigma(\alpha)$ curves derived at a constant force (Figure 5a) and a constant strain rate (Figure 4a) indicates that the strain rates are very close at the points of their intersection. To corroborate this fact use was made of the $\kappa(\alpha)$ curves obtained at extension with F = const (see Figure 6). These

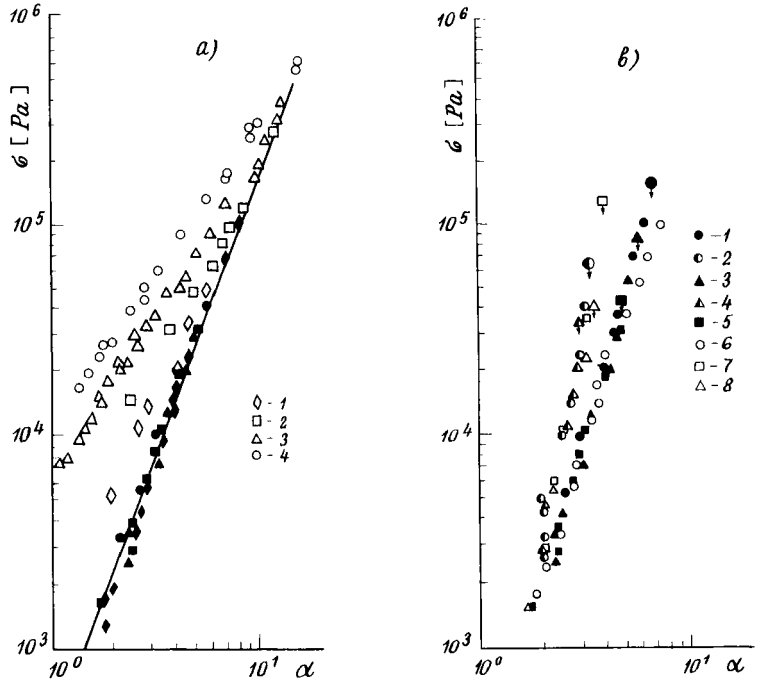

FIGURE 5 (a) Tensile stress σ versus recoverable strain α at extension with a constant force. Corresponding to points 1 through 4 are σ_0 = (1, 3.3, 6.3, 11.7)·10³ N/m². Black symbols represent the envelope for these relationships. (b) Stress σ versus α in the case of stress relaxation after extension. Corresponding to points 1 and 2 are $\sigma_0 = 11.7 \cdot 10^3$ N/m² and $\ln \varepsilon = 3.4$ and 1.8; corresponding to points 3 and 4 are $\sigma_0 = 6.3 \cdot 10^3$ N/m² and $\ln \varepsilon = 3.4$ and 1.8; corresponding to point 5 are $\sigma_0 = 3.3 \cdot 10^3$ N/m² and $\ln \varepsilon = 3.4$; corresponding to point 6 is the envelope derived in the case of extension at a constant strain rate; and corresponding to points 7 and 8 are $\kappa = 10^{-1}$ and $1.2 \cdot 10^{-2}$ and $\ln \varepsilon = 1.8$.

curves have been plotted for different values of σ_0 from the data presented in Figure 3a, b.

The black symbols and the line passing through them in Figures 4a and 5a represent the envelope. The manner in which it has been derived is illustrated by Figures 4b and 5b.

Figures 4b and 5b represent $\sigma(\alpha)$ curves corresponding to stress relaxation either after extension with a constant strain rate or after extension of a constant force. The black symbols with arrows correspond to the points (σ, α) at which the process of relaxation begins. Consider now how the $\sigma(\alpha)$ curves have been derived.

Under the stress relaxation condition where stress $\sigma(t)$ was measured (preceded by extension of the specimen), the specimen was cut at different instants t, and recoverable strain α was measured. Naturally, the stress relaxation

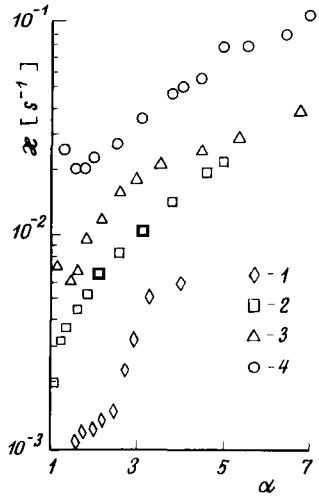

FIGURE 6 Strain rate κ versus recoverable strain α at extension with a constant force. Corresponding to points 1 through 4 are σ_0 = (1, 3.3, 6.3, 11.7)·10^3 N/m^2.

process was discontinued at that moment and had to be repeated for taking the next value of α. Thus, the $\alpha(t)$ curve was obtained during stress relaxation. The $\sigma(t)$ and $\alpha(t)$ curves are represented in Figure 7. As these curves were derived, the stress relaxation was preceded by extension at F = const and κ = const up to a strain of 5.8 (ln ε = 1.8). Similar curves were obtained for other values of ε. The $\sigma(t)$ and $\alpha(t)$ curves obtained during stress relaxation were used in plotting the $\sigma(\alpha)$ curves shown in Figures 4b and 5b.

It should be emphasized once again that in order to obtain the $\sigma(\alpha)$ curves presented in Figure 4b, the stresses in the specimen extended at κ = const were relaxed, while the curves of Figure 5b are the result of relaxation after extension at F = const (with the exception of points 6 to 8 which have been transferred from Figure 4b for comparison).

As can be inferred from Figures 4b and 5b, the relaxation curves $\sigma(\alpha)$ coincide if the relaxation is initiated at the points (σ, α) lying on the common curve (see, for example, points 2, 4, 7 and 8 in Figure 5b). Note that total strain ε at these points is approximately the same. In this case, it is immaterial under what conditions the points corresponding to the onset of relaxation (black symbols with arrows) have been obtained. For example, points 2 and 4 in Figure 5b have been obtained at a constant force, whereas points 7 and 8 (transferred from Figure 4b) have been obtained at a constant strain rate.

The resulting relaxation curves $\sigma(\alpha)$ converge into an envelope (see Figures 4b and 5b) which is the same for both extension conditions (see points 6 in

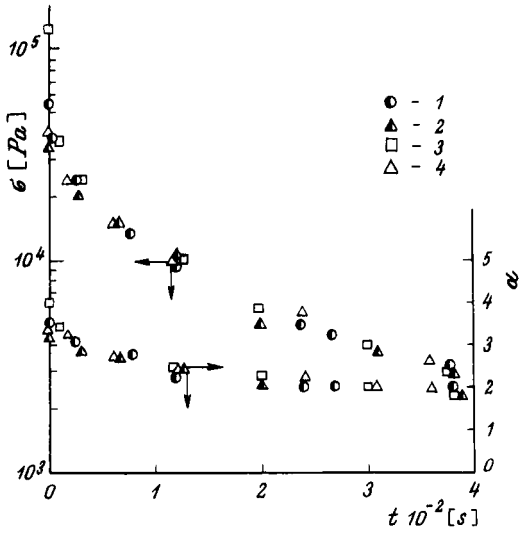

FIGURE 7 Stress σ and recoverable strain α versus time t in the case of relaxation after extension with κ = const and F = const up to strain ε = 5.8 (ln ε = 1.8). Corresponding to points 1 and 2 are $\sigma_0 = 11.7 \cdot 10^3$ and $6.3 \cdot 10^3$ N/m^2; and corresponding to points 3 and 4 are $\kappa = 10^{-1}$ and $1.2 \cdot 10^{-2}$ s^{-1}.

Figure 5b transferred from Figure 4b). This is precisely the envelope represented in Figures 4a and 5a by black symbols and line. Note that the $\sigma(\alpha)$ curves derived in the case of extension at κ = const and F = const lie to the left of the envelope.

A procedure similar to that considered for $\sigma(\alpha)$ was repeated for $e_p(\alpha)$. In this case, too, a respective envelope has been obtained.[5]

It should be pointed out that the knowledge of the envelope of the $\sigma(\alpha)$ curve (with due account for the strength properties of the polymeric liquid[10]) gives an insight into the limitations imposed at any extension of an elastic liquid on recoverable strain α which is a measure of orientation.

The experiments under consideration are also of interest in elaborating and corroborating theories of the kind described in Ref. 6, in which the dependence of stress on recoverable strain is explicit. The solution of respective problems as proposed in Ref. 6 and comparison of the results with the presented experimental data have revealed a satisfactory quantitative fit.[5]

3. NONUNIFORM EXTENSION

In experiments with nonuniform steady-state extension use was made of the arrangement shown in Figure 8. Cylindrical specimen 2 in contact with pulley

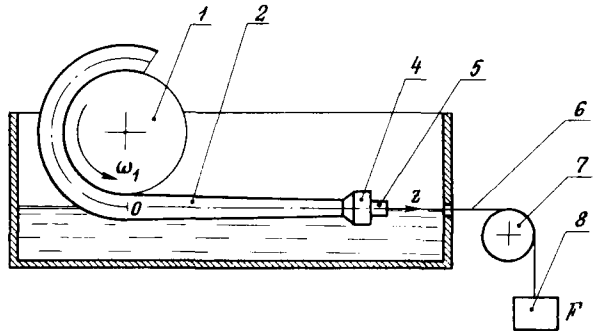

FIGURE 8 Setup for nonuniform extension with a constant force.

of radius R (attached its own of adhesion) gradually detached itself at a constant angular velocity from the pulley as the latter was rotating and was stretched with constant force F. The stretched specimen stayed afloat. Force F was created by a weight with a thread passing through the pulley just as in uniform extension experiments (see Section 2.2).

Nonuniform drawing is easier to achieve by stretching (with force F) a liquid squeezed out of a capillary. But even this case involves some phenomena which are beyond control and create difficulties in experimentation, namely: the shear stress in the capillary may distort the drawing pattern; the tensile stress may detach the polymer from the capillary walls; as the polymer fills the bulb of the capillary viscometer, air bubbles may form in it.

Let us introduce a system of cylindrical coordinates z, r and ϕ, axis z extending along the stretched specimen (see Figure 8). Place the origin of coordinates ($z = 0$) at the point of detachment of the specimen from the pulley. Let $r(z)$ and V_z be the radius and longitudinal velocity of the liquid under extension. Assume that $|r'| = |dr/dz| < 1$ and that for the components of stress σ and strain rate κ tensors, under conditions of slightly nonuniform steady-state drawing, the total derivative with respect to time d/dt approximated by expression

$$\frac{d}{dt} \approx V_z \frac{\partial}{\partial z}. \tag{10}$$

In this case,[7,8] tensors σ and κ are diagonal up to the terms of the r'-th order (the stress tensor component different from zero is $\sigma = \sigma_{zz} = F/\pi r^2$), and the velocity components at $V_z|_{z=0} = V_1$ are as follows:

$$V_z = V_1 + \int_0^z \kappa(z)\, dz; \qquad V_r = -\frac{\kappa(z)}{2}; \qquad V_\phi \equiv 0,$$

where V_z, V_r and V_ϕ are the velocity vector components and κ is the strain

rate. In this case, it was assumed that the polymer specimen on the rotating pulley is, up to point $z = 0$, in a non-strained state (the validity of this assumption is considered in discussion of the experiments).

Taking the above assumptions as regards nonuniform extension with $F = \text{const}$ into consideration, we see that every cross section of the specimen, normal to the z axis, is strained with time t, as it moves along the z axis, just as in the case of uniform extension with the same force. Therewith, corresponding to $t = 0$ are $z = 0$ and $r/_{t=0} = r/_{z=0} = r_0$.

The relationship between strain time t at uniform extension and coordinate z at nonuniform extension is as follows

$$z = \int_0^{t(z)} V_z(t)\,dt = V_1 \int_0^t \varepsilon(t_1)\,dt. \tag{11}$$

This relationship is derived from Exps. (10) and (3) taking into account that

$$V_z = q/\pi r^2 = V_1(r_0/r)^2 = V_1 \frac{l}{l_0} = V_1\varepsilon, \tag{12}$$

where q is the flow rate, $V_1 \approx \omega_1 R$ is the jet velocity at $z = 0$, and ε is the total longitudinal strain.

The profile of the liquid under nonuniform extension (the $r(z)$ curve) is calculated from Exp. (11) and from the following expression for the radius:

$$r = r_0\varepsilon(t)^{-1/2}. \tag{13}$$

This expression follows from Exp. (3). The $\varepsilon(t)$ curve is found experimentally (or theoretically) at uniform extension with a constant force (see Figure 3a).

By residual length z_r at nonuniform extension is here meant the length attained by the elastically contracted stretched specimen after elastic contraction, cut at points 0 and z at the same time (in the case of elastic recovery, $\sigma \equiv 0$). The corresponding values are in the following relationship at uniform extension:

$$z_r = \int_0^z \frac{d\xi}{\alpha\xi} = V_1 \int_0^t \frac{\varepsilon(t_1)}{\alpha(t_1)}\,dt_1, \tag{14}$$

where α is the recoverable strain at uniform extension with a constant force. Equation (14) has been derived from Exps. (5), (10) and (12). Relationship $z_r(z)$ is calculated from the experimental data obtained at uniform extension (see Figure 3), namely from Exps. (14) and (11). Also note that $z/z_r \neq \alpha(z)$ is independent of V_1, as can be inferred from Exps. (11) and (14).

The experiment aimed at verifying the obtained relationships (in determining dr/dz at which these relationships hold) was conducted using a melt of polyisobutylene P-20 at 22°C. The same polymer, as was mentioned in Section 2.2, was used in the uniform extension experiments.

The uniform drawing yielding experimental data necessary for the calculations was carried out at $\sigma_0 = 6.3 \cdot 10^3$ N/m^2 using the arrangement illustrated

in Figure 1 and discussed at length in Section 2.2. Stress σ_0 was preset by means of a weight corresponding to 0.18 N. The initial length of the specimen was $l_0 = 2$ to 5 cm, and the initial radius was $r_0 \approx 0.3$ cm.

The curves representing $\varepsilon = l/l_0$ and $\alpha = l/l_r$ versus time t for $\sigma_0 = 6.3 \cdot 10^3$ N/m^2, independent of l_0, are indicated by dots 3 in Figure 3.

In the case of nonuniform extension using the arrangement of Figure 8 at $z = 0$, the polymer was detached from the pulley by means of a razor blade and a weight corresponding to 0.18 N, just as in the case of uniform extension. Radius R of the pulley was 4 cm. The initial radius of the specimen was $r/_{z=0} = r_0 \approx 0.3$ cm and equal to that in the case of uniform extension at $t = 0$. The specimen moved through point $z = 0$ at $V_1 = 2.13 \cdot 10^{-4}$, $1.07 \cdot 10^{-4}$ and $0.54 \cdot 10^{-4}$ m/s. The profile of the specimen was obtained by photography to 1:1 scale. The elastic recovery time in measuring z_r (for determination of z_r see above) was taken the same as in uniaxial extension (see Section 2.2).

The extension under investigation was a steady-state one. The deformation of the polymer on the pulley started slightly upstream of point $z = 0$ (at a distance of 1 to 2 cm from the latter). The strain propagated along the specimen on the pulley as the value of V_1 decreased.

The calculation curves representing r/r_0 and r_r/V_1 versus z/V_1, obtained from the experimental data of Figure 3 for $\sigma_0 = 6.3 \cdot 10^3$ N/m^2 and Exps. (11), (13) and (14), are given in Figure 9 (curves 1 and 2, respectively). Here and in what follows, no mention is made of similar curves at low values of t because of their being not accurate enough.

The experimental values of r/r_0 obtained at $V_1 = 1.07 \cdot 10^{-4}$ m/s are represented in Figure 9 by dots 2. In the region slightly different from $z = 0$ ($z > 0$), a good agreement between the experimental and calculation data is observed. In this case, the value of derivative $dr/dz = -(r_0/V_1)(\kappa/\varepsilon^{2/3})$ becomes as high as -0.05, which exceeds the values normally observed in practice. Some discrepancy between the calculation and experimental data is observed in the neighborhood of $z = 0$, which seems to be due to the strain reaching the region of $z < 0$.

The experimental points $(z_r/V_1, z/V_1)$ are indicated in Figure 9 by black symbols and have been obtained for different values of V_1. These dots form a single curve independent of V_1 and agreeing well with the calculated relationship (see Exps. (11) and (14)).

For greater assurance the $z(t)$ relationship was also verified directly (see Exp. (11)). During the experiment, a line was painted on the specimen at a right angle to the z axis, and the movement of this line along the latter was observed in time ($t = 0 \leftrightarrow z = 0$). The white symbols in Figure 9 stand for the experimental values of z/V_1 as a function of t for different values of V_1. The maximum value of z measured at these speeds is 12.7, 6.35 and 3.2 cm,

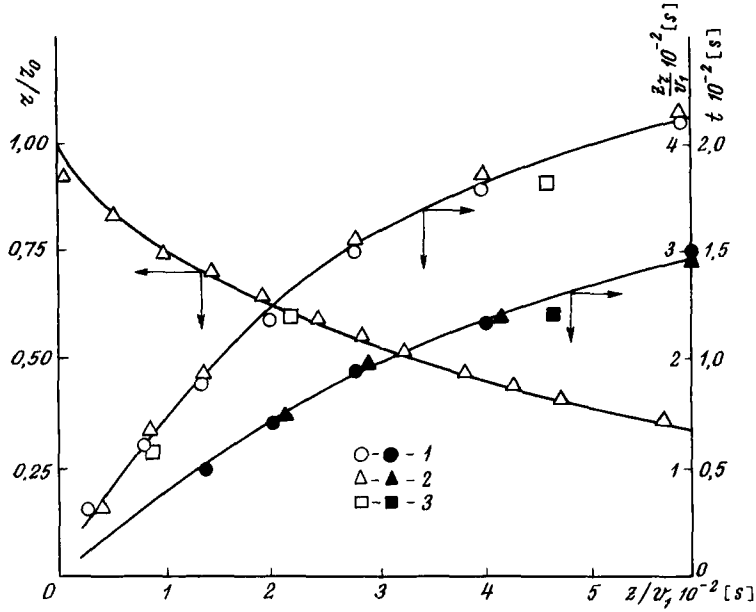

FIGURE 9 Nonuniform extension with $\sigma_0 = 6.3 \cdot 10^3$ N/m^2. r/r_0 and z_r/V_1 versus z/V_1 (curves 1 and 2) and z/V_1 versus t (curve 3). Corresponding to points 1 through 3 are $V_1 = (2.13, 1.07, 0.54) \cdot 10^{-4}$ m/s.

respectively. The radius of the specimen, corresponding to these lengths, was reduced more than three times. Curve 3 in Figure 9 represents the relationship derived from Exp. (11) and Figure 3a. z/V_1 as a function of t is independent of V_1. At $V_1 = 0.54 \cdot 10^{-4}$ m/s, the dots appear to depart somewhat from the curve, which is probably due to deformation of the specimen on the pulley at $z < 0$.

Consider now another case where nonuniform steady-state extension is attained not by using a weight but by means of a second pulley having radius R and rotating at angular velocity $\omega_2 (\omega_2 \geqslant \omega_1)$. The distance between the centers of both pulleys is L. The second pulley imparts the specimen constant speed $V_z(L) = V_2 \approx \omega_2 R$. The set of curves representing V_z/V_1 versus z/V_1 at different values of σ_0 (derived from the experimentally found $\varepsilon(t)$ curves at different values of σ_0 and from Exps. (11) and (12)) are used to obtain a relationship at which $V_z(L/V_1)/V_1 = V_2/V_1$. Determined in this manner is σ_0, hence the jet profile, stress $\sigma(z) = \sigma_0 V_z/V_1$, and recoverable strain $\alpha(z)$.

In many instances (see, for example, Ref. 9), particularly in the case of low-viscosity liquids, value $\eta^*(z) = \sigma(z)/\kappa(z)$ determined at nonuniform steady-state extension for a fixed value of z is treated as viscosity $\eta_1^* = \sigma/\kappa$ at uniform steady-state extension with $\kappa = \kappa(z) = \text{const}$. As can be inferred

from the above relationship between nonuniform and uniform extensions with a constant force ($z \leftrightarrow t$; $\kappa(z) \leftrightarrow \kappa(t)$; $\sigma(z) \leftrightarrow \sigma(t)$) and from the above figures, equality $\eta_1^* = \eta^*$ does not always hold. A most striking example where the assumption from Ref. 9 is not always valid involves extension at an experimental temperature below the yield point. In this case, we cannot speak of steady extension with $\kappa = \text{const}$, hence, viscosity η_1^*; what we have in fact is nonuniform steady-state extension.

Going from uniform extension (which in some cases can be experimentally achieved without any difficulties) to the nonuniform one (which is prevalent in various production processes) may be useful in analysis of the following phenomena: strength properties of liquids,[10] the effect of straining in a capillary (nozzle) on subsequent extension, non-isothermal drawing, etc.

4. POLYMERIC LIQUID FLOW RETARDATION UNDER LARGE RECOVERABLE STRAIN

Uniform extension at a constant strain rate is used as an example in considering the retardation of flow of a polymeric liquid after its fully developed flow.

Most experiments were conducted using a low-density polyethylene (molecular weight, *ca.* 10^5) in the temperature range of 125 to 150°C. The crystallization temperature is $T_{cr} = 113$°C. Polyethylene, which is transparent in the molten state, becomes turbid when cooled to a lower temperature. The initial viscosity at 125°C is $\eta = 3.10^6$ p, the relaxation time being $\theta \sim 10^2$ s (determined from the time it takes to attain steady flow at shear strain with $\kappa = \text{const}$ in the region of linear behavior of the liquid).

Extension at $\kappa = \text{const}$ was carried out on a setup with a variable specimen length.[2] Silicone oil was used as the thermostatic fluid.

Cylindrical specimens with diameter $d = 2r_0 \simeq 0.5$ cm were prepared by squeezing the polymer out of a capillary viscosimeter.

Measured in the experiments were tensile force F, recoverable strain $\ln \alpha$ and nonrecoverable strain $\ln \beta$. To provide for appropriate retardation conditions (for measuring l_r), the specimens were cut with scissors.

Note that preheating over a long period of time might decrease the values of $F(t)$ to some extent. Therewith, the basic shape of the $F(t)$ curves remained the same (at 2-hr long heating). It has been established that no changes occur when the specimen is heated for 15 to 30 minutes; this period of time is quite sufficient for preheating the specimen prior to testing since heating time $t \sim d^2/a \approx 2.5 \cdot 10^2$ s ("a" being the temperature conductivity coefficient equal to 0.1 mm^2/s for polyethylene).

The scatter of the experimental data with respect to F did not exceed

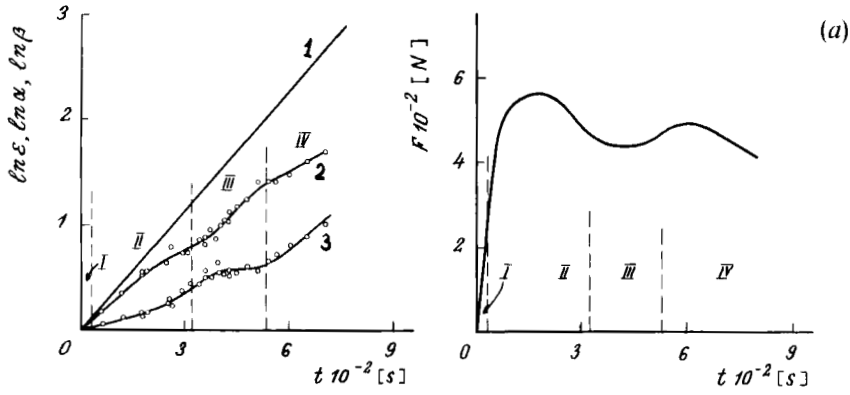

FIGURE 10 Total strain ln ε(1), recoverable strain ln α(2), nonrecoverable strain ln β(3) and tensile force F versus time t for low-density polyethylene in the case of extension with κ = const. (a) $\kappa = 3.84 \cdot 10^{-3}$, (b) $1.2 \cdot 10^{-2}$, and (c) 0.1 s^{-1}.

$\pm 8\%$ (the graphs represent averaged lines), and the scatter with respect to ln α and ln β can be seen from the experimental points in the graphs.

Figure 10 represents experimental curves of tensile force F, recoverable strain ln α and nonrecoverable strain ln β versus time t at 125°C. The straight line also stands for total strain ln $\varepsilon = \kappa t$ (see Figure 10). At $\kappa = 3.84 \cdot 10^{-3}$ and $1.2 \cdot 10^{-2}$ s^{-1} (see Figure 10a, b), four strain regions are defined.

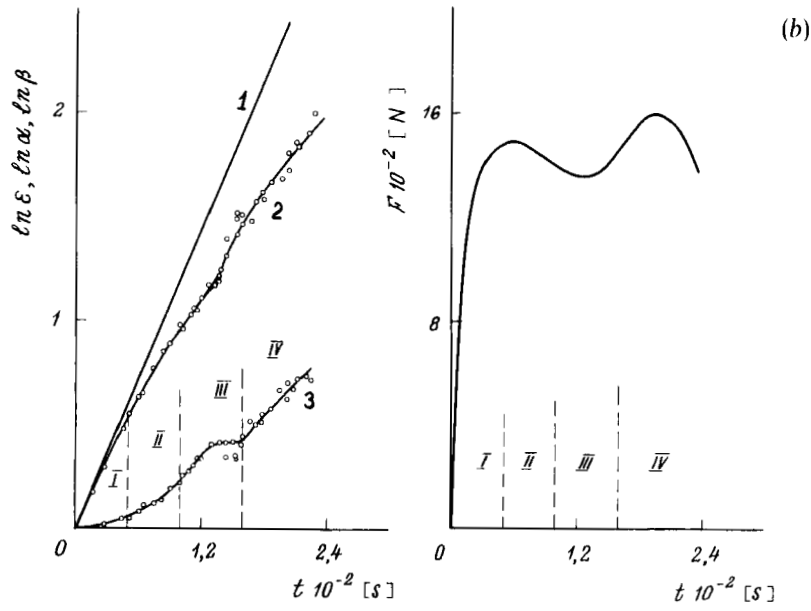

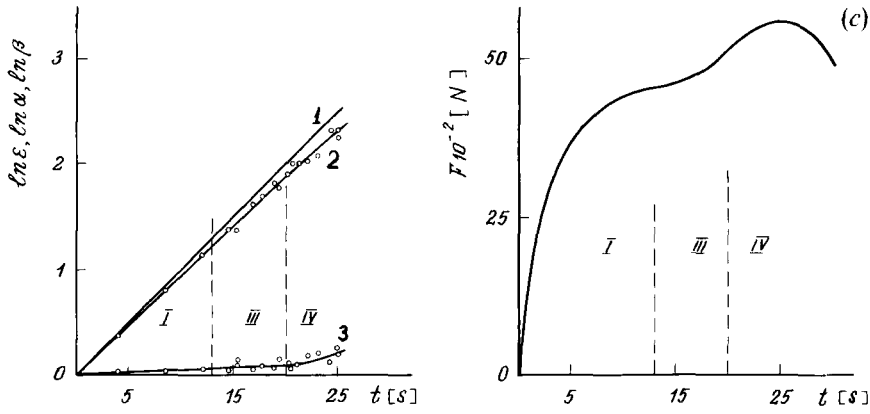

Region I, which starts with instant $t = 0$, is characterized by a slight difference between recoverable strain ln α and total strain ln ε (e.g. less than 5%). The strain time in region I is much shorter than the relaxation time, and the polymer is strained similarly to a solid. In this region, force $F(t)$ grows.

In region II, the flow of the polymeric medium develops (e_p (see Exp. (7)) increases). In this region, force $F(t)$ passes through a maximum and then starts to decrease.

Region III begins with the flex point on the downsloping portion of the $F(t)$ curve. This point corresponds to the flex point on the upsloping portion of the ln β curve. In this region, the rate of nonrecoverable strain e_p starts decreasing with increasing t and approaches zero (ln $\beta \approx$ const), i.e. the nonrecoverable strain is suppressed in this region and the polymer starts to be strained similarly to a solid. In this case, the force repeatedly increases in the neighborhood of $e_p \approx 0$, which is also typical of straining of solids in the case of major recoverable strains at $\kappa = \text{const}$.

In the region IV, the flow develops again ($e_p > 0$). Note that in all of the four regions the polymer remains equally transparent and is uniformly strained.

At $\kappa = 0.1\ s^{-1}$ (Figure 10), the minimum on the $F(t)$ curve disappears, and the first increase in force is immediately followed by another (region II is practically absent). Thus, the recoverable strain region at times shorter than the relaxation time merges with the region of secondary solidification.

Note that in all of the above-considered cases, the second increase in force is followed by its decrease accompanied by the development of secondary flow. Straining in the region of secondary flow produces practically no irreversible effect on the polymer. This was verified by comparing the $F(t)$

curves derived using specimens prepared from a polymer after it had been involved in secondary flow and unstrained specimens.

Stress σ (see Exp. (2)) at extension with $\kappa \geqslant 1.2 \cdot 10^{-3}$ s^{-1} increases monotonically in time when the force both increases and decreases. Note that when the force increases the increase in stress σ is not slower than exp κt (see Exp. (8)). At $\kappa < 1.2 \cdot 10^{-3}$ s^{-1}, the $\sigma(t)$ curves could not be obtained because of the considerable errors in tensile force measurements.

The $\sigma(t)$ curves derived at shear flow normally reach a constant value in the course of time (steady-state shear flow). In shear experiments, use was made of a Wissenberg rheogoniometer up to $\kappa = 0.5$ s^{-1}.

The experiments have shown that, when extension and shear occur at temperatures above the crystallization point (125 to 150°C), the $F(t)$ curves are temperature-invariant.[11]

Two maxima on the $F(t)$ curve were also observed in experiments with extension of a high-density polyethylene melt. Following the second increase in $F(t)$ for this polymer, the specimen broke after necking down. A second increase in force immediately following the first (as shown in Figure 10c) was also observed in the case of a noncrystallizable polymer, *viz.* polystyrene melt. In stretching these two polymers, the amount of recoverable strain was not measured.

Hence, a polymeric liquid may feature two regions during straining, in which it is deformed similarly to a solid. One of these regions occurs at relatively low strains (when the strain time is much shorter than the relaxation time), and the other region occurs at high strains. Both regions may merge into one. The flow retardation (solidification) during extension at a constant strain rate is followed by an increase in the tensile force. After the secondary solidification either secondary flow occurs or the material breaks. Systematic studies into breaks caused by extension of melts are described in Ref. 10. Note that breaks may also occur, in principle, in the range of strain times shorter than relaxation times and have nothing to do with the secondary solidification region. If the secondary solidification is treated in terms of another increase in the tensile force, then it can be maintained that this property is typical of polymeric liquids of different nature.

When polyisobutylene was stretched (see Section 2) in the examined range of strain rates and temperatures, the $F(t)$ curves featured a single maximum followed by a monotonic decrease. Consequently, in order to observe a secondary increase in force in this case greater strain rates must be achieved.

In conclusion, we should like to point out that the principal equations[6] are based on the polymer's ability to solidity at high recoverable strains. In the case of extension at $\kappa = \text{const}$, this property results in that $e_p \to 0$ with increasing t[5], i.e. starting from a certain moment the polymer must elongate like a solid. Possibly, the solidification considered in this work and else-

where[5,6] is of the same nature (entropic). In this case, the basic difference of the theory expounded in Ref. 6 resides in that the experimentally observed solidification occurs only within a limited space of time. The secondary flow following the solidification may be due, for example, to the stress-induced distortion of the potential barriers determining the activation process.

Acknowledgement

The author acknowledges with gratitude and affection the generous help he has received from Professor G. V. Vinogradov in writing this paper.

References

1. G. V. Vinogradov, A. I. Leonov and A. N. Prokunin, *Rheol. Acta*, **8,** 482 (1969).
2. G. V. Vinogradov, B. V. Radushkevich and V. D. Fikhman, *J. Polymer Sci., A-2*, **8,** 1 and 657 (1960).
3. M. S. Akutin, A. N. Prokunin, N. G. Proskurnina and O. Yu. Sabsai, *Meckhanika Polimerov*, **2,** 353 (1977).
4. H. M. Laun and H. Munstedt, *Rheol. Acta*, **15,** 517 (1976).
5. A. N. Prokunin, Nonlinear elastic phenomena under the extension of polymeric liquids. Experiment and theory. Preprint N 104, Institute for Problems in Mechanics AN SSSR (1978).
6. A. I. Leoniv, *Rheolog. Acta*, **15,** 517 (1976).
7. V. G. Litvinov, *Mekhanika Polimerov*, **2,** 326 (1967).
8. A. I. Leonov and A. N. Prokunin, Izvestiya AN SSSR, *Mekhanika Zhidkosti i Gaza*, **5,** 24 (1973).
9. V. N. Pokrovsky, N. P. Kruchikhin, G. A. Danilin and A. T. Serkov, *Mekhanika Polimerov*, **1,** 124 (1973).
10. G. V. Vinogradov, *Polymer*, **18,** 1275 (1977).
11. G. V. Vinogradov and A. Ya. Malkin, *Prikladnaya Mekhanika i Tekhnicheskaya Fizika*, **5,** 25 (1964).